ChaMPlane Galactic Bulge Latitude Survey: Optical Results

Ping Zhao, Jonathan E. Grindlay, Jaesub Hong, Mathieu Servillat & Maureen van den Berg

Harvard-Smithsonian Center for Astrophysics
Cambridge, MA 02138 U.S.A.

Silas Laycock

Gemini Observatory, Hilo, HI 96720 U.S.A.

http://hea-www.harvard.edu/ChaMPlane/

ABSTRACT

We present the initial optical result of the Galactic Bulge Latitude Survey (BLS), which is an important component of our ChaMPlane survey (see Grindlay et al.). It extends from ± 0.2 to ± 1.6 degrees along the galactic latitude, centered at the SgrA*. The main goal is to measure the radial gradient of the Lx $> 10^{31.5}$erg/s source population (primarily CVs and qLMXBs) along latitude vs. longitude in the galactic bulge. We completed the BLS survey in Chandra cycles 7-10, with 36 ACIS-I pointings of 15ks each. The survey covers two 1.2 square-degrees region in the "north" (BLS-N) and "south" (BLS-S) of the galactic plane. The southern tip of the BLS-S is connected with our Chandra observation "Limiting Window", a low extinction window closest to the SgrA* with Av=3.9. We also completed the corresponding optical and IR (see van den Berg et al.) survey to cover the same region. The optical images (V,R,I,Hα band) were obtained from CTIO/4m/Mosaic from 2008 to 2009. Six Mosaic images ($36' \times 36'$) covers all 36 Chandra pointings. Candidate optical counterparts of the X-ray point sources were found from the Mosaic images. Here we present the results of photometry, X-ray – optical matching, and source distribution of the BLS survey. Spectroscopic follow-ups for the identified optical counterparts were conducted in 2009 using the CTIO/4m/Hydra for classification, to identify the nature of the Chandra sources (these results will be presented in the near future).

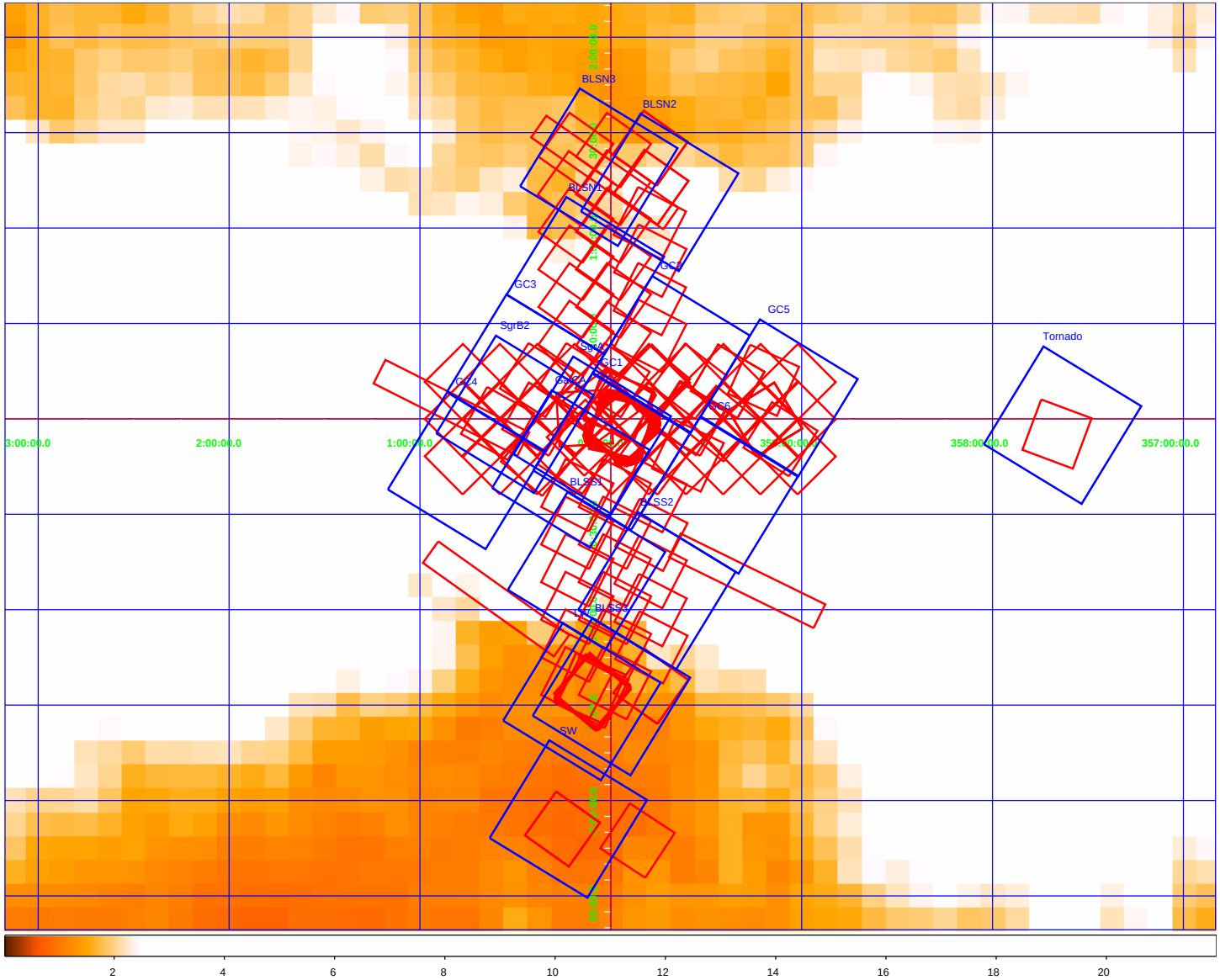

Figure 1: ChaMPlane survey, overlays on extinction (E_{B-V}) map, in the Galactic center ($6^\circ l \times 4^\circ b$): Mosaic fields (blue squares), ACIS-I (red squares), ACIS-S (red rectangles)

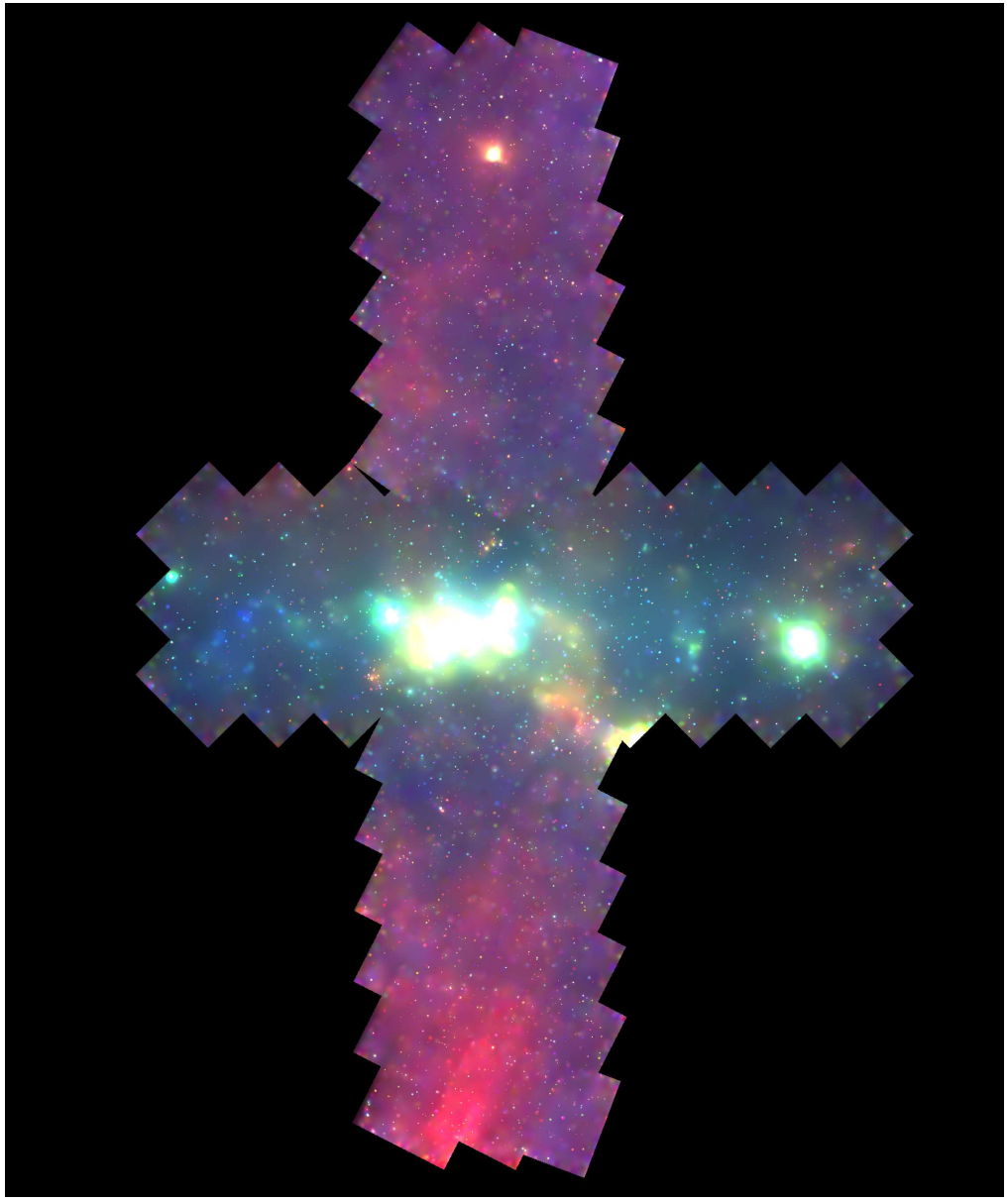

Figure 2: BLS (PI: Grindlay) + GCS (PI: Wang) survey: red (soft: 1-3keV), green (medium: 3-5 keV), blue (hard: 5-8keV)

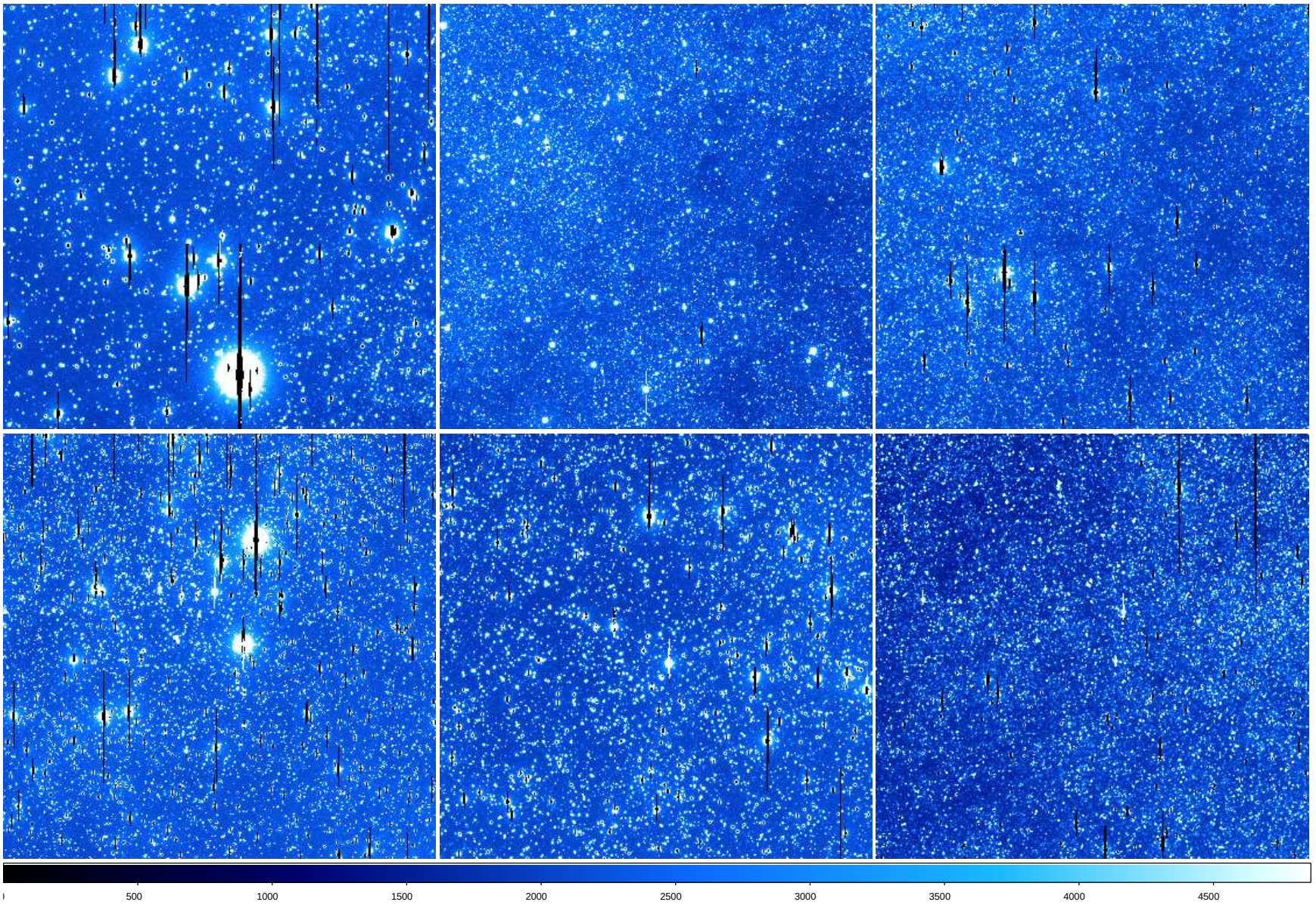

Figure 3: ChaMPlane Budge Latitude Survey optical R band Mosaic images. Top row: BLSN1, BLSN2, BLSN3. Bottom row: BLSS1, BLSS2, BLSS3. Visible star densities become higher as the images move away from the the plane, due to lesser extinction. FoV: $10' \times 10'$, North-right, east-up.

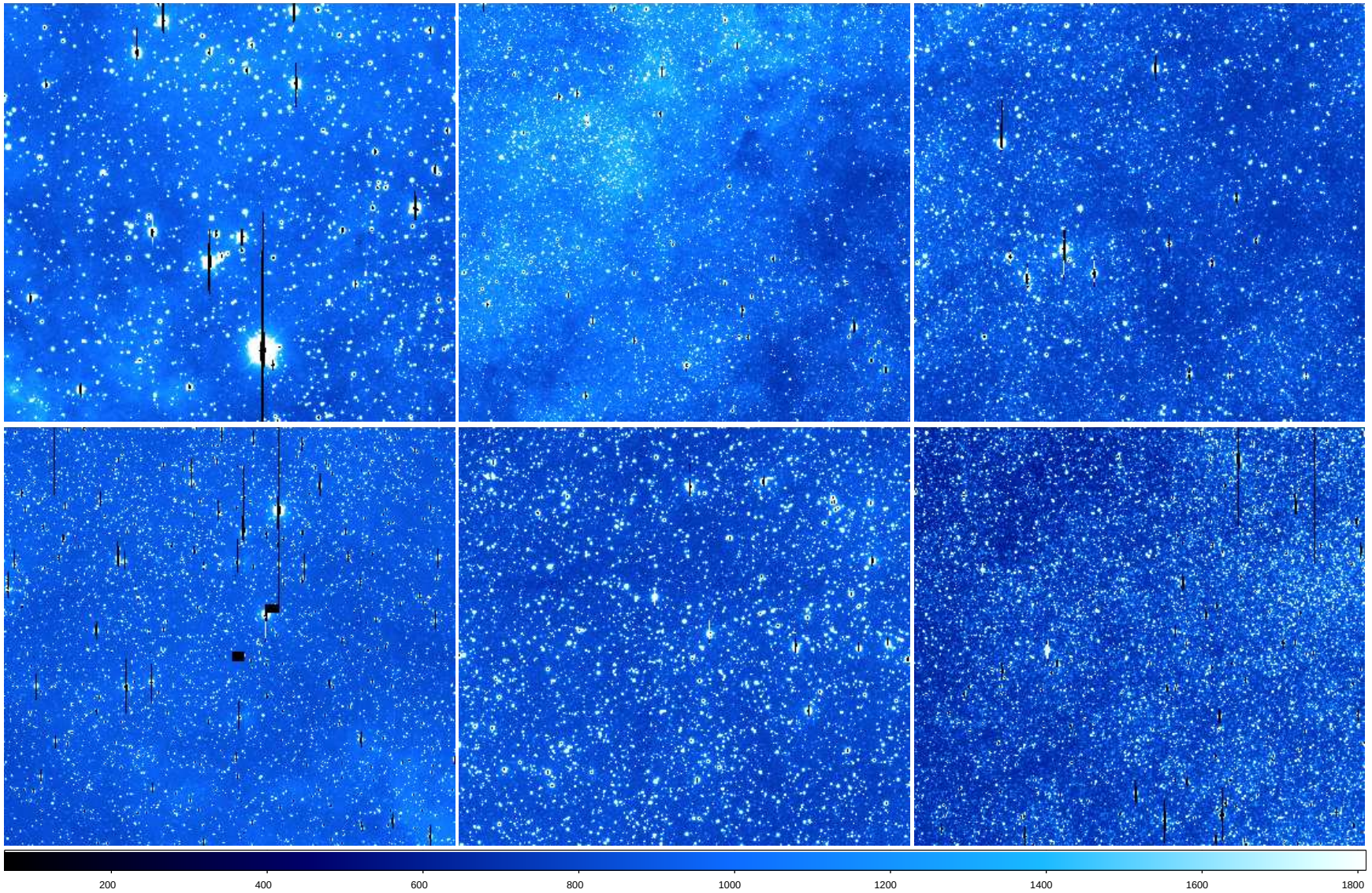

Figure 4: ChaMPlane Budge Latitude Survey Optical Hα band Mosaic images. Top row: BLSN1, BLSN2, BLSN3. Bottom row: BLSS1, BLSS2, BLSS3. Visible star densities become higher as the images move away from the the plane, due to lesser extinction. FoV: $10' \times 10'$, North-right, east-up.

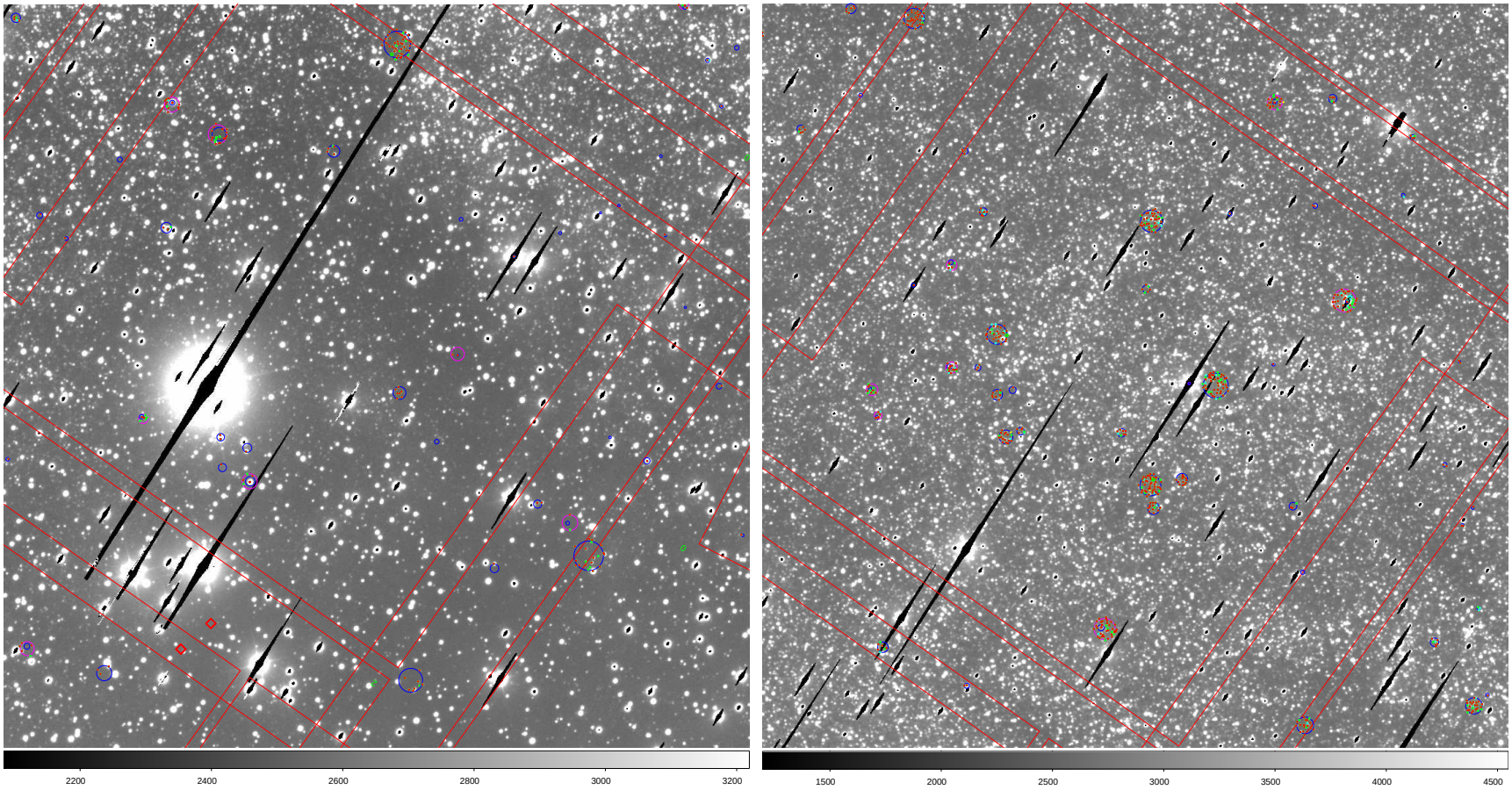

Figure 5: BLSN1 (left) and BLSN3 (right) Mosaic R band images with X-ray source error circles (blue or magenta) and their optical matches (red, green or cyan). FoV: $10' \times 10'$**, Galactic north-up, east-left.**

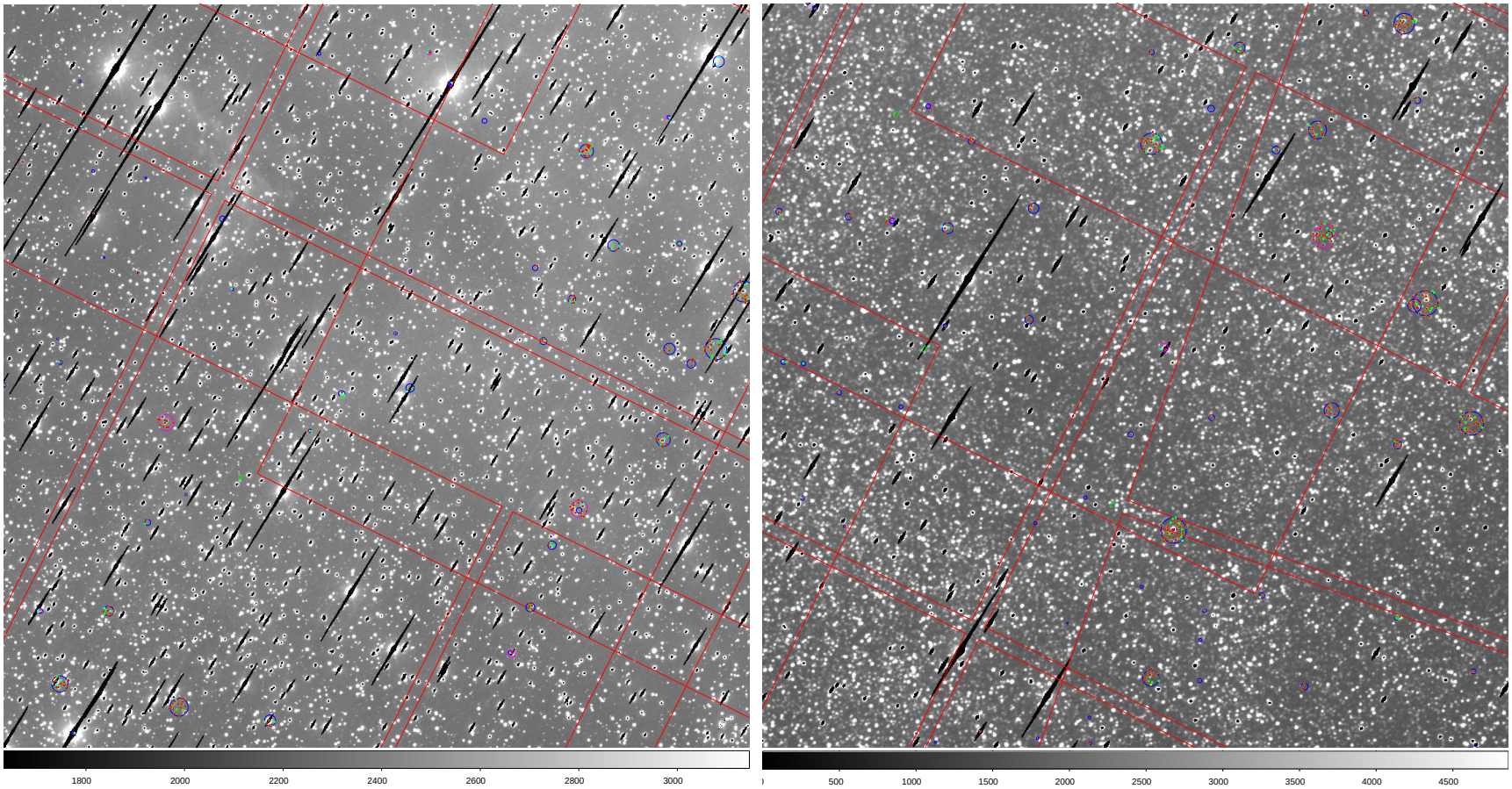

Figure 6: BLSS1 (left) and BLSS3 (right) Mosaic R band images with X-ray source error circles (blue or magenta) and their optical matches (red, green or cyan). FoV: $10' \times 10'$**, Galactic north-up, east-left.**

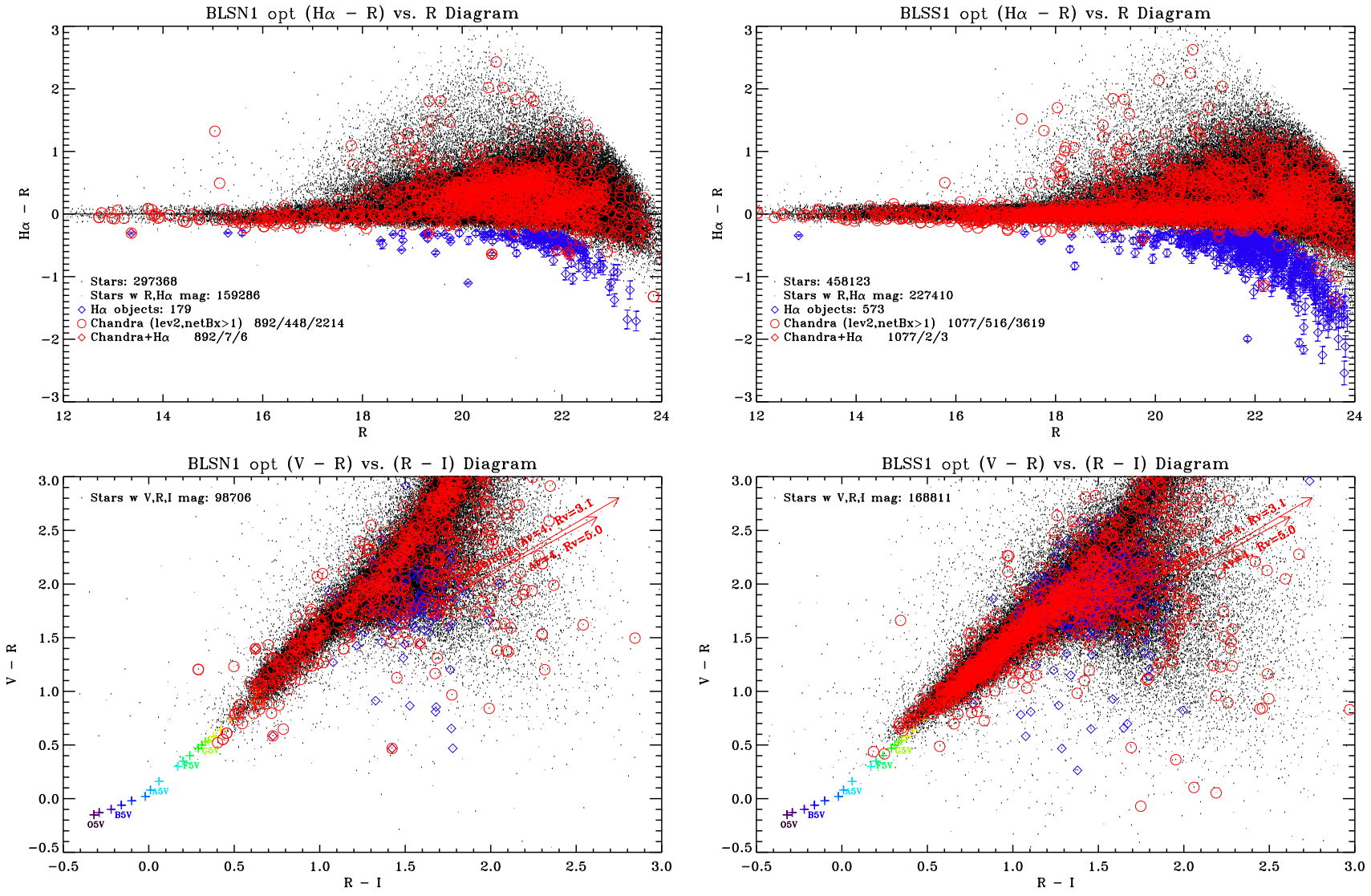

Figure 7: Results of BLSN1 (left) and BLSS1 (right) fields: $(H\alpha - R)$ vs. R color-magnitude (top) and $(V - R)$ vs. $(R - I)$ color-color (bottom) diagrams. $H\alpha$ emission sources ($H\alpha - R < -0.3$ and $S/N > 5$) and X-ray optical counterparts are found in the Mosaic images.

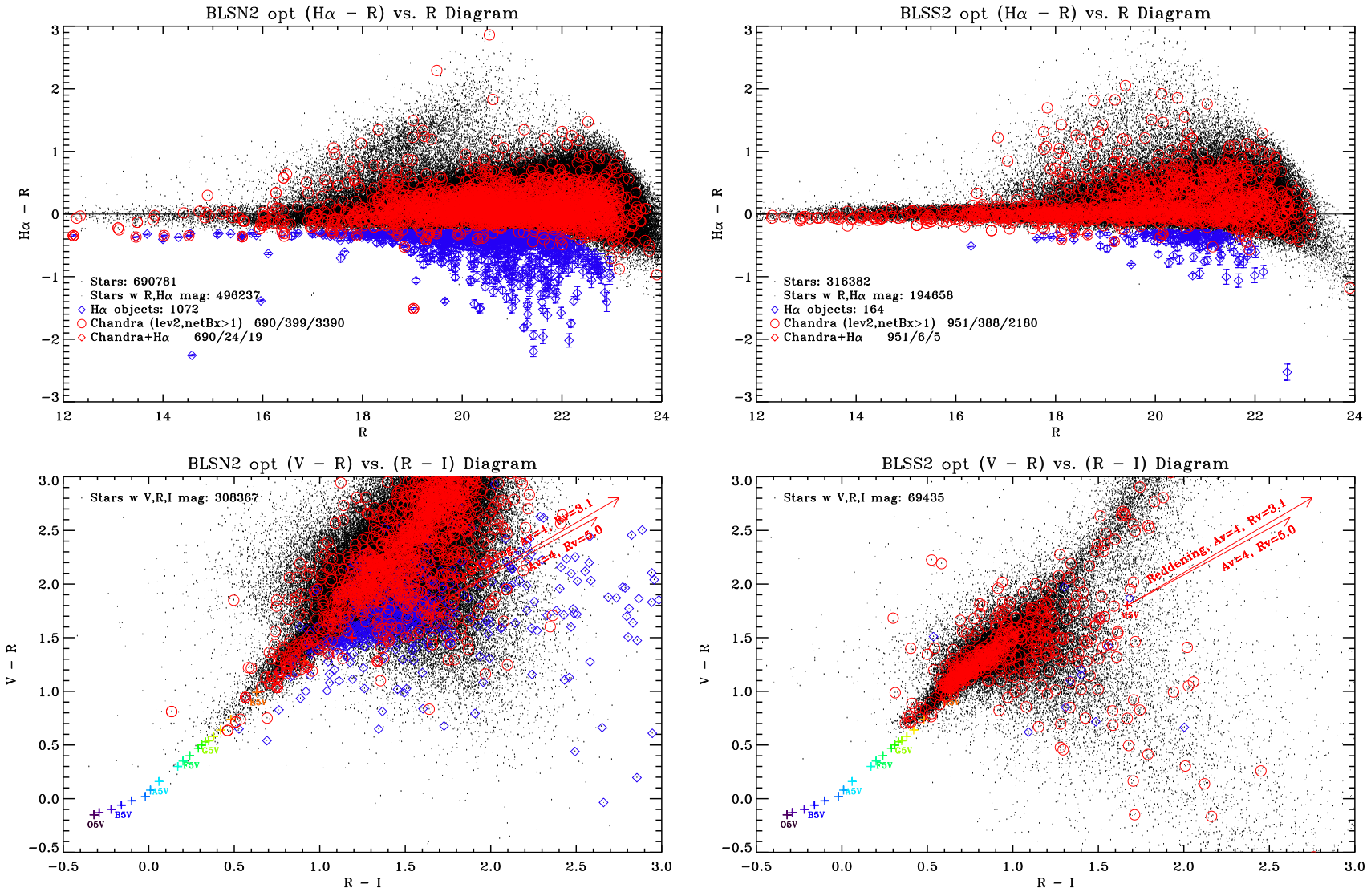

Figure 8: Results of BLSN2 (left) and BLSS2 (right) fields: $(H\alpha - R)$ vs. R color-magnitude (top) and $(V - R)$ vs. $(R - I)$ color-color (bottom) diagrams. Hα emission sources ($H\alpha - R < -0.3$ and S/N > 5) and X-ray optical counterparts are found in the Mosaic images.

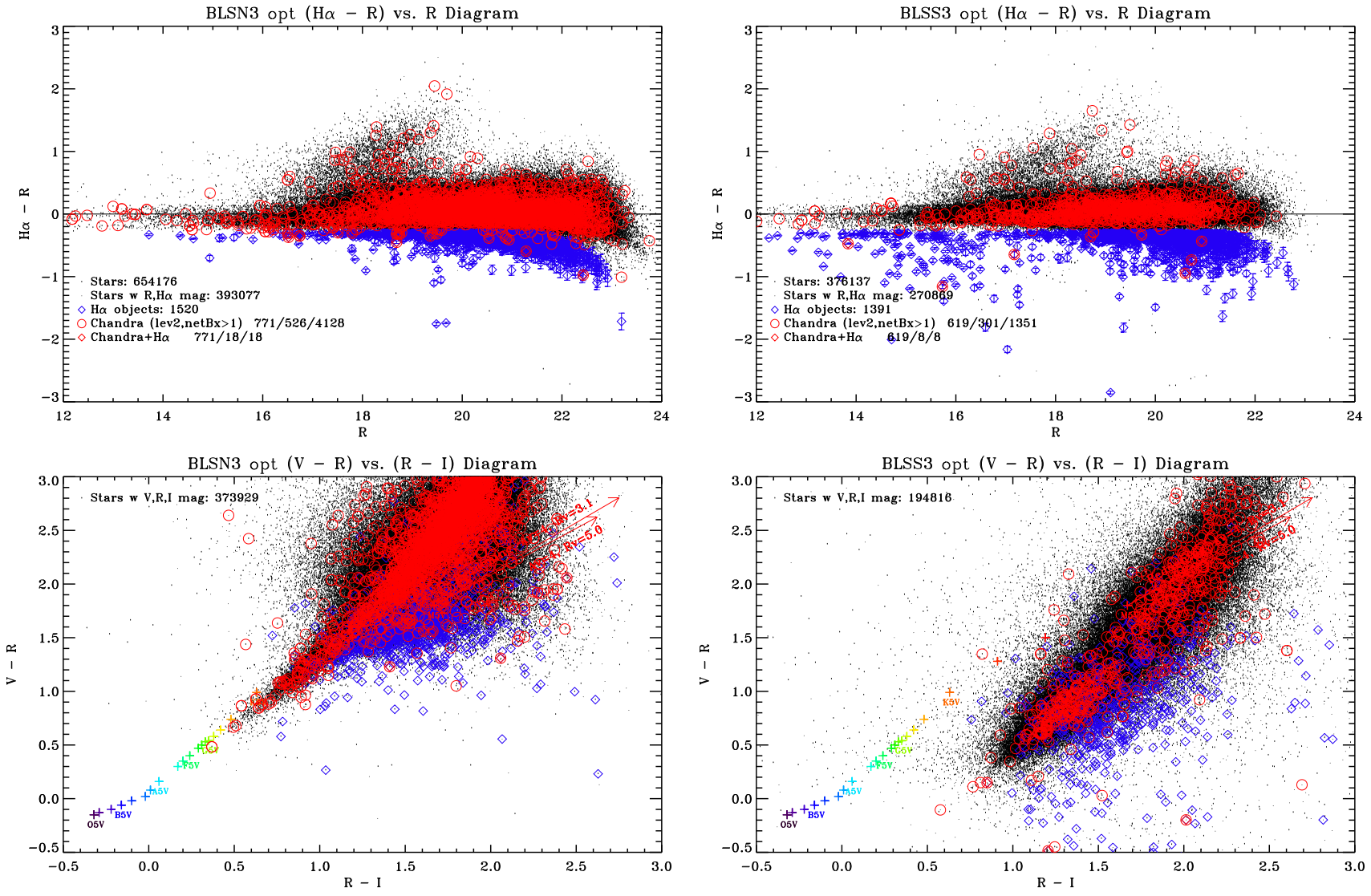

Figure 9: Results of BLSN3 (left) and BLSS3 (right) fields: $(H\alpha - R)$ vs. R color-magnitude (top) and $(V - R)$ vs. $(R - I)$ color-color (bottom) diagrams. Hα emission sources ($H\alpha - R < -0.3$ and $S/N > 5$) and X-ray optical counterparts are found in the Mosaic images.

BLSN1 Field Chandra Source Coincident Matches: level $\geq$ 2, xmatch $\geq$ 1

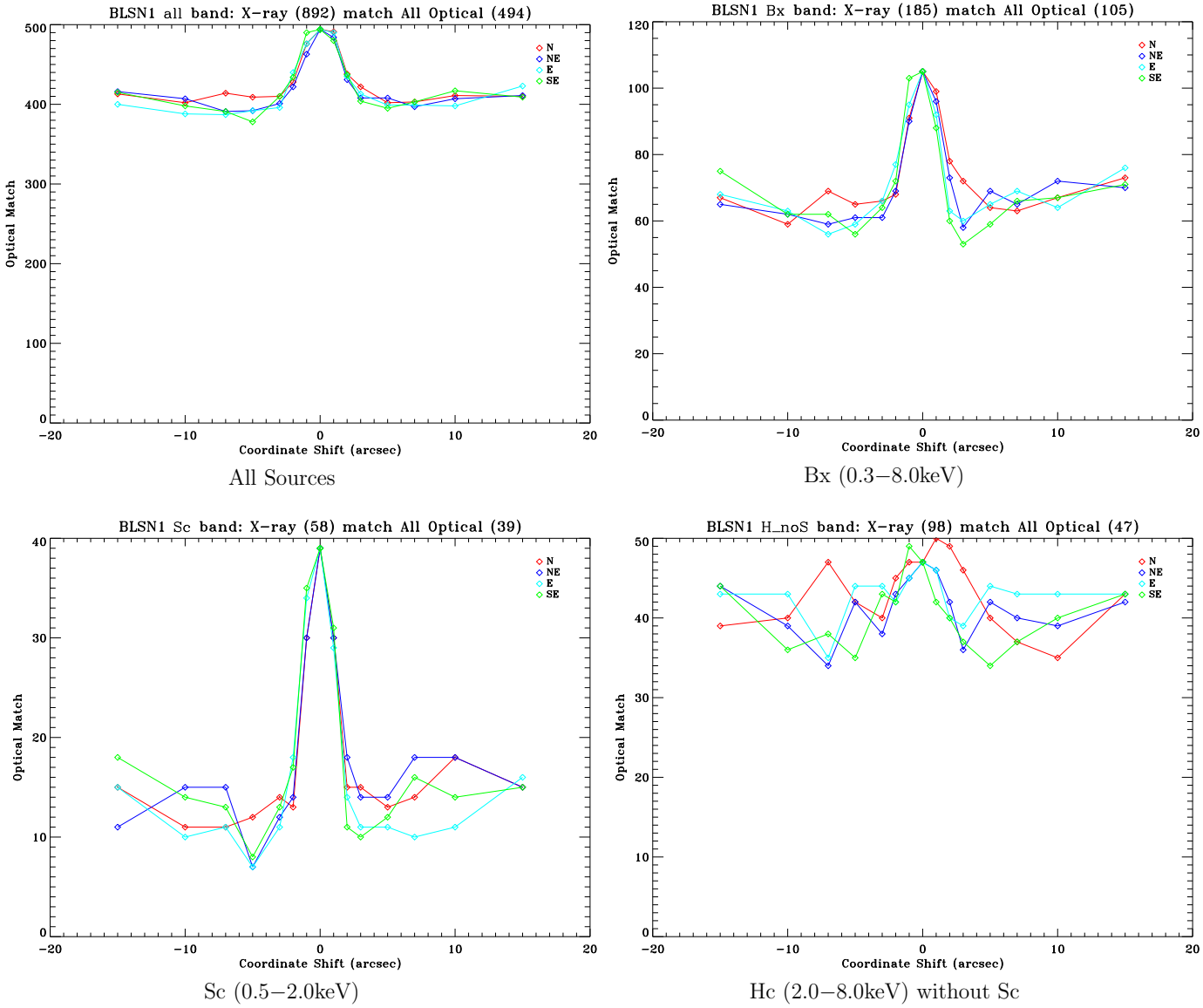

Figure 10: BLSN1 field Chandra source optical counterpart coincident match test: Soft band sources (lower-left) peak at the origin, indicating good real match. Hard band sources (lower-right) have no peak, indicating random match with foreground stars.

BLSN2 Field Chandra Source Coincident Matches: level $\geq$ 2, xmatch $\geq$ 1

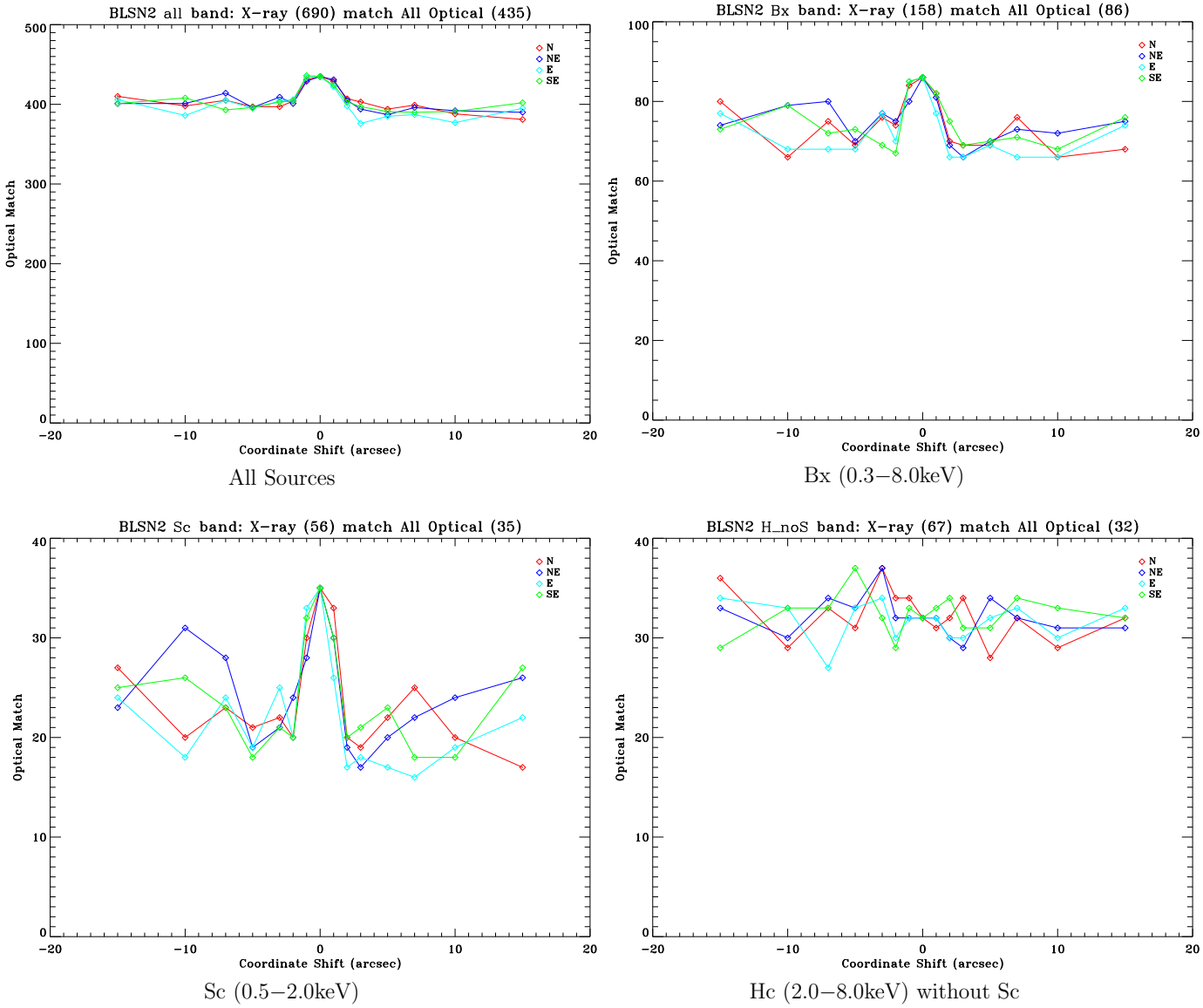

All Sources | Bx (0.3−8.0keV)

Sc (0.5−2.0keV) | Hc (2.0−8.0keV) without Sc

Figure 11: BLSN2 field Chandra source optical counterpart coincident match test: Soft band sources (lower-left) peak at the origin, indicating good real match. Hard band sources (lower-right) have no peak, indicating random match with foreground stars.

BLSN3 Field Chandra Source Coincident Matches: level $\geq$ 2, xmatch $\geq$ 1

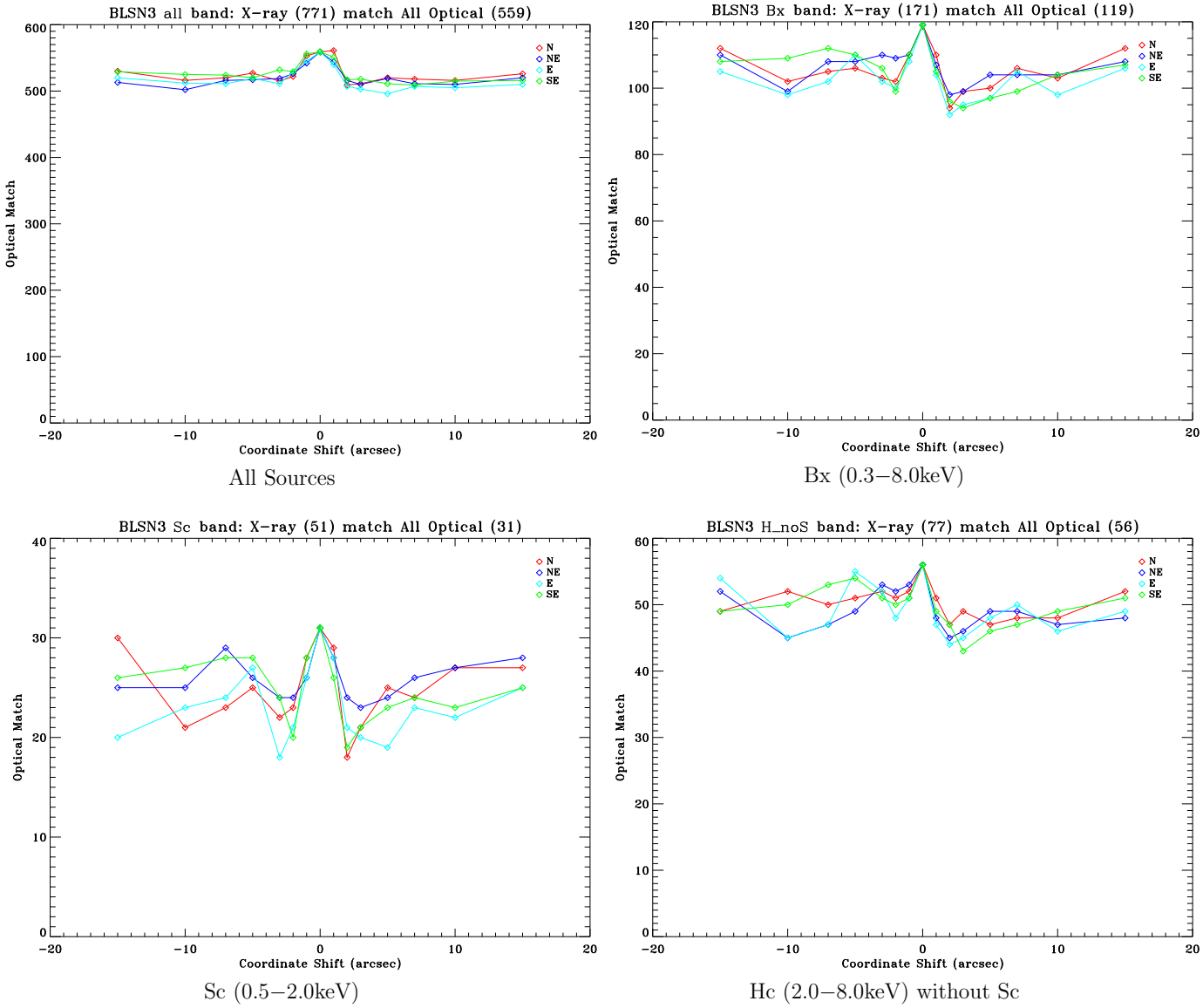

Figure 12: BLSN3 field Chandra source optical counterpart coincident match test: Soft band sources (lower-left) peak at the origin, indicating good real match. Hard band sources (lower-right) have no peak, indicating random match with foreground stars.

BLSS1 Field Chandra Source Coincident Matches: level $\geq$ 2, xmatch $\geq$ 1

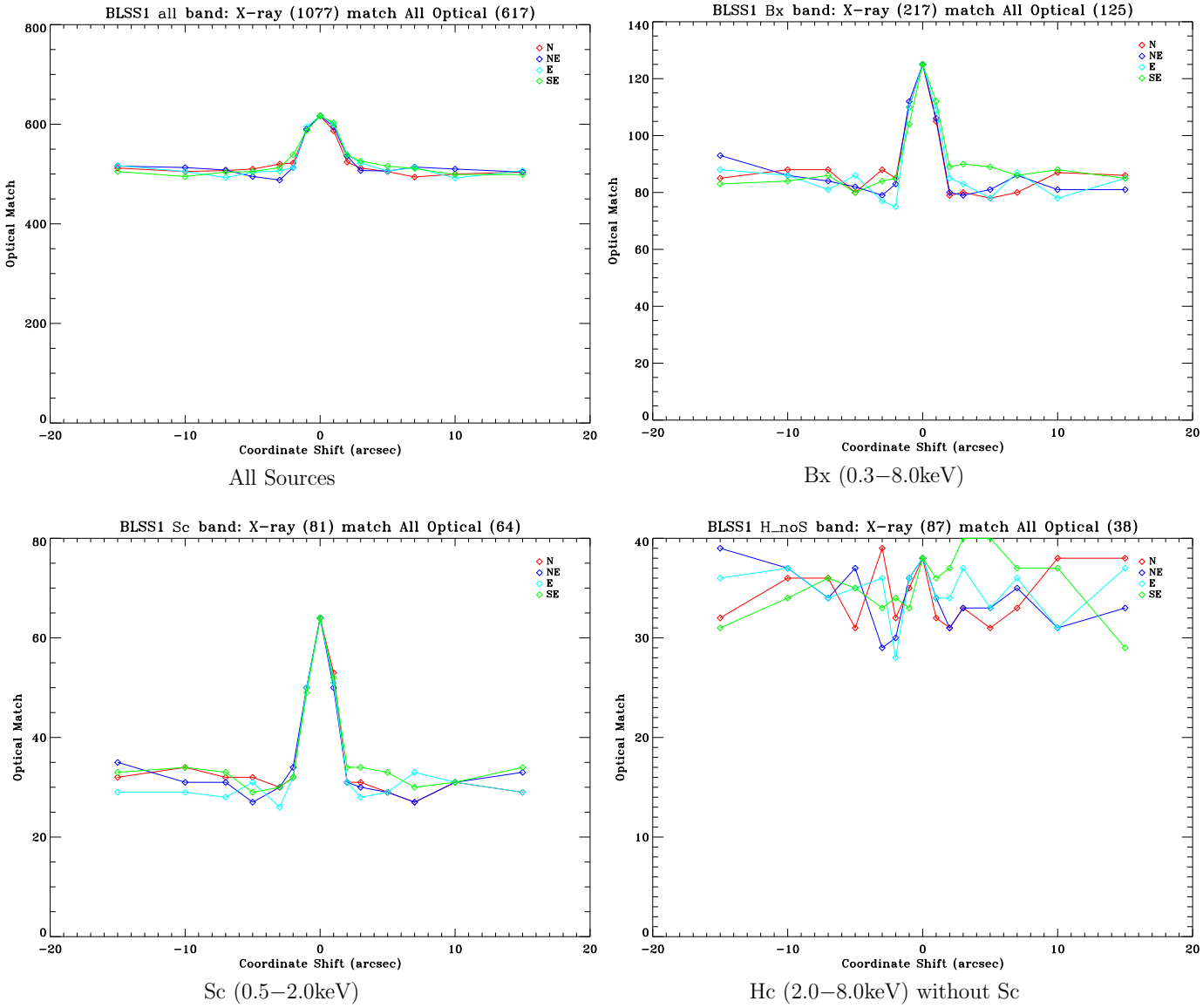

Figure 13: BLSS1 field Chandra source optical counterpart coincident match test: Soft band sources (lower-left) peak at the origin, indicating good real match. Hard band sources (lower-right) have no peak, indicating random match with foreground stars.

BLSS2 Field Chandra Source Coincident Matches: level $\geq$ 2, xmatch $\geq$ 1

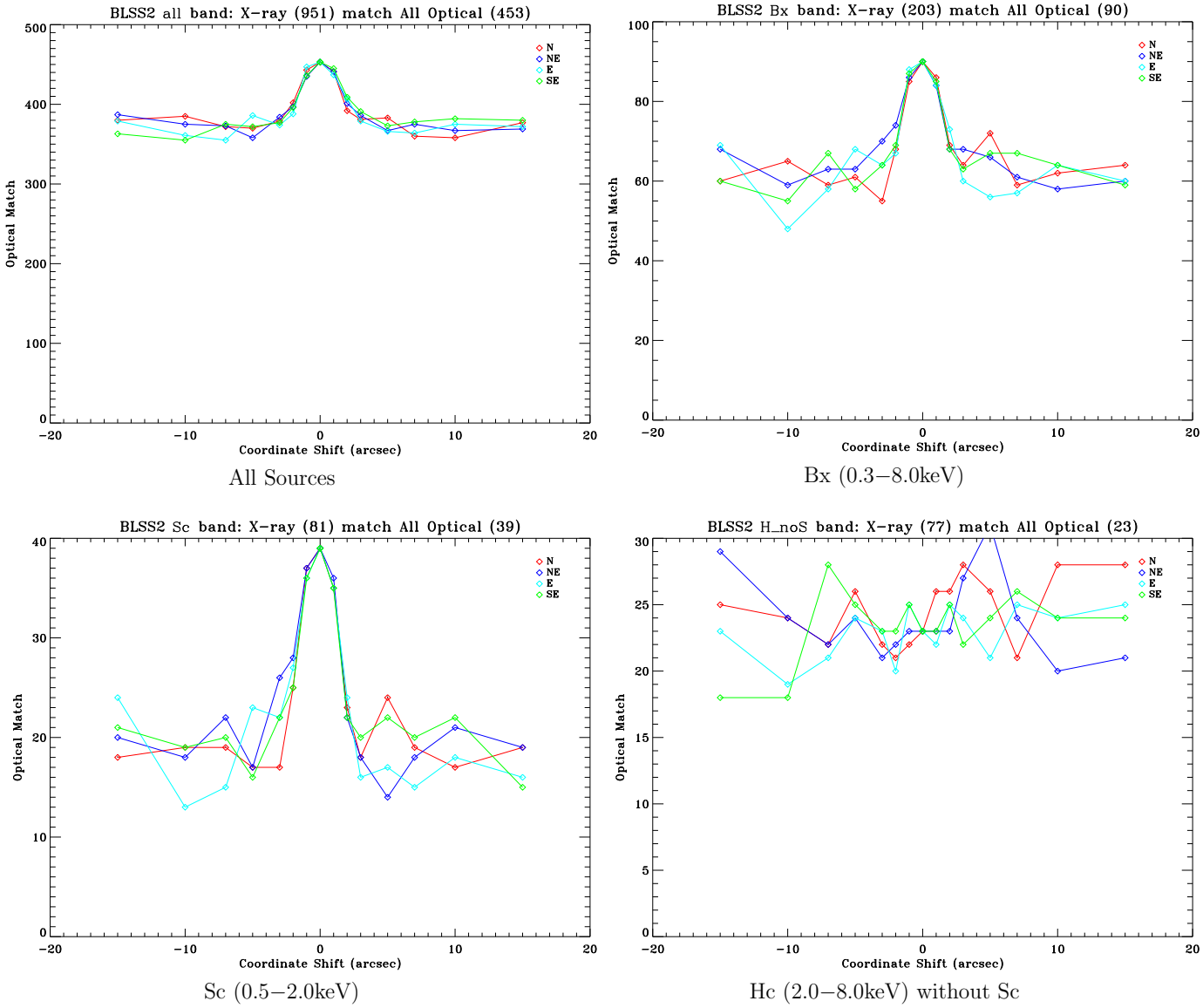

All Sources | Bx (0.3−8.0keV)

Sc (0.5−2.0keV) | Hc (2.0−8.0keV) without Sc

Figure 14: BLSS2 field Chandra source optical counterpart coincident match test: Soft band sources (lower-left) peak at the origin, indicating good real match. Hard band sources (lower-right) have no peak, indicating random match with foreground stars.

BLSS3 Field Chandra Source Coincident Matches: level $\geq$ 2, xmatch $\geq$ 1

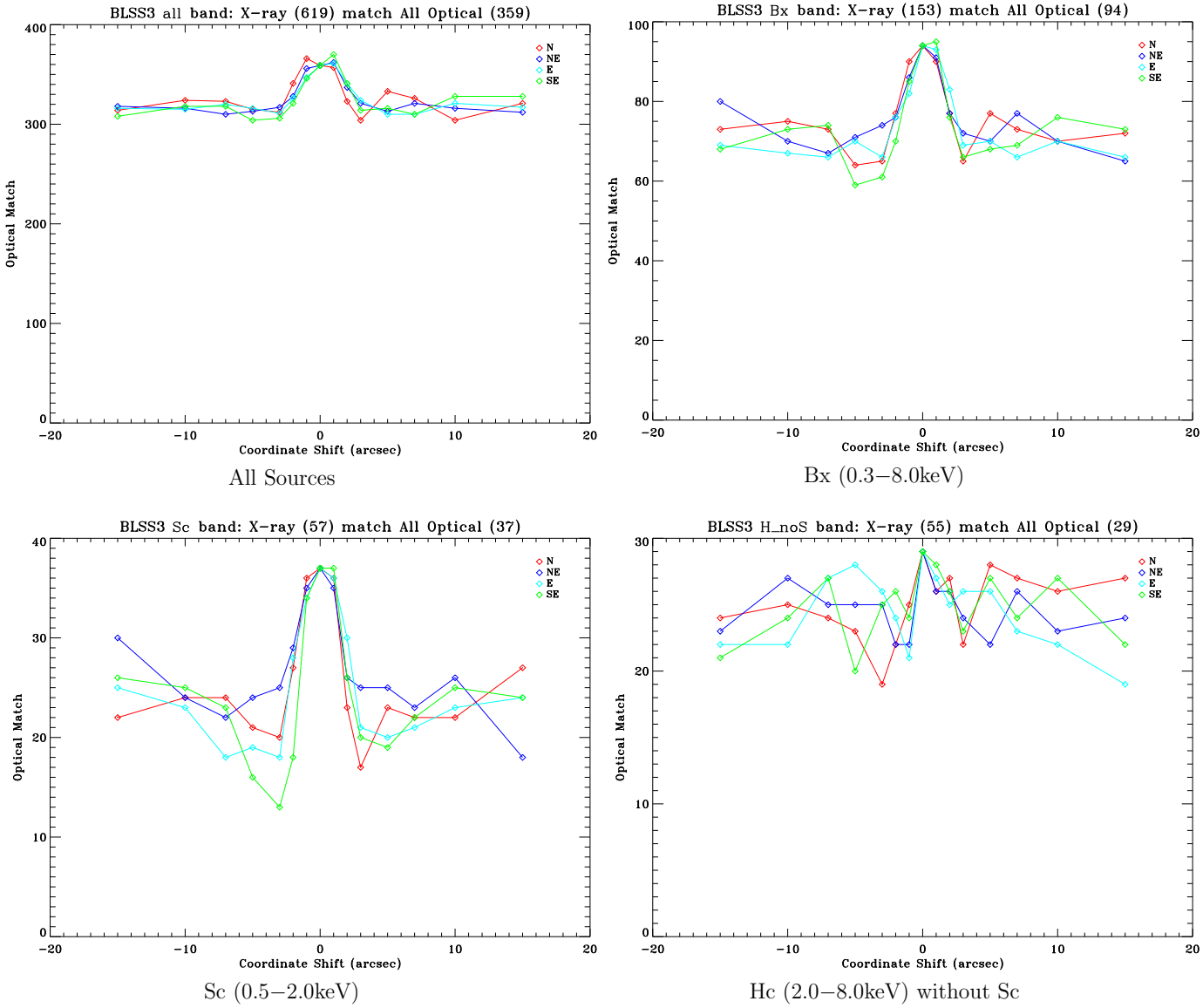

All Sources | Bx (0.3−8.0keV)

Sc (0.5−2.0keV) | Hc (2.0−8.0keV) without Sc

Figure 15: BLSS3 field Chandra source optical counterpart coincident match test: Soft band sources (lower-left) peak at the origin, indicating good real match. Hard band sources (lower-right) have no peak, indicating random match with foreground stars.

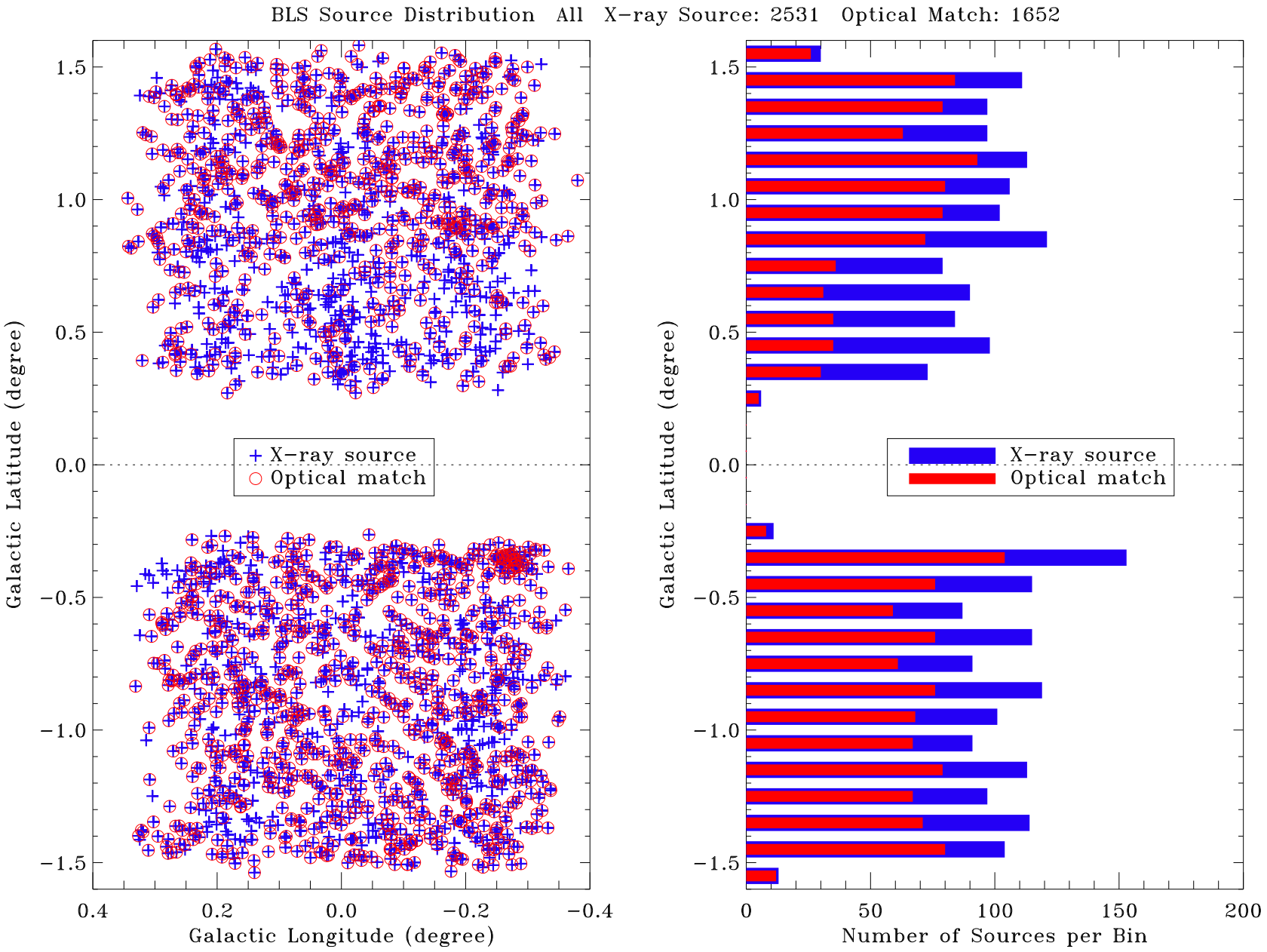

Figure 16: BLS source distribution: All the sources with netBx≥1.

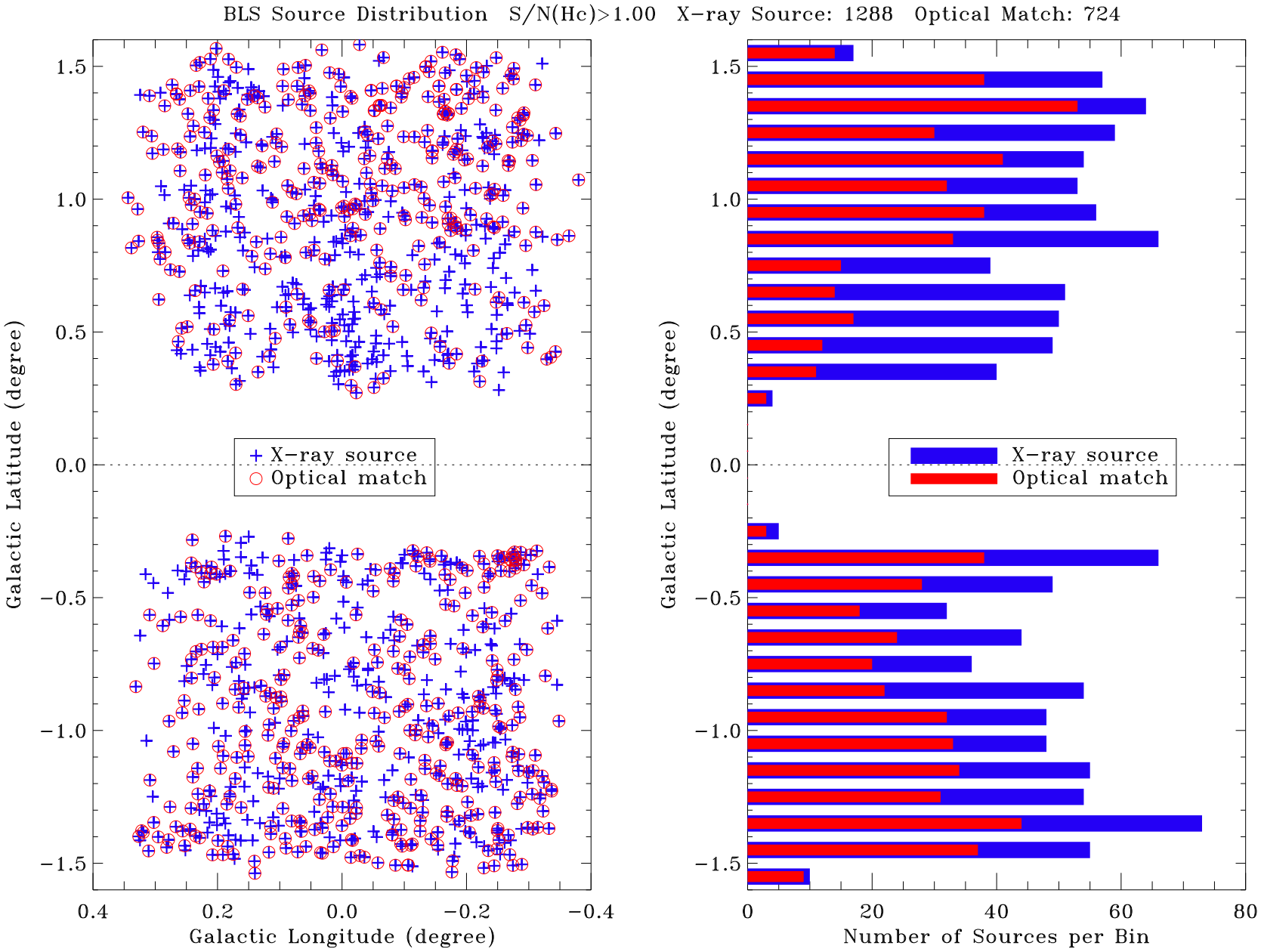

Figure 17: BLS source distribution: Hc (2.0-8.0keV) band sources.

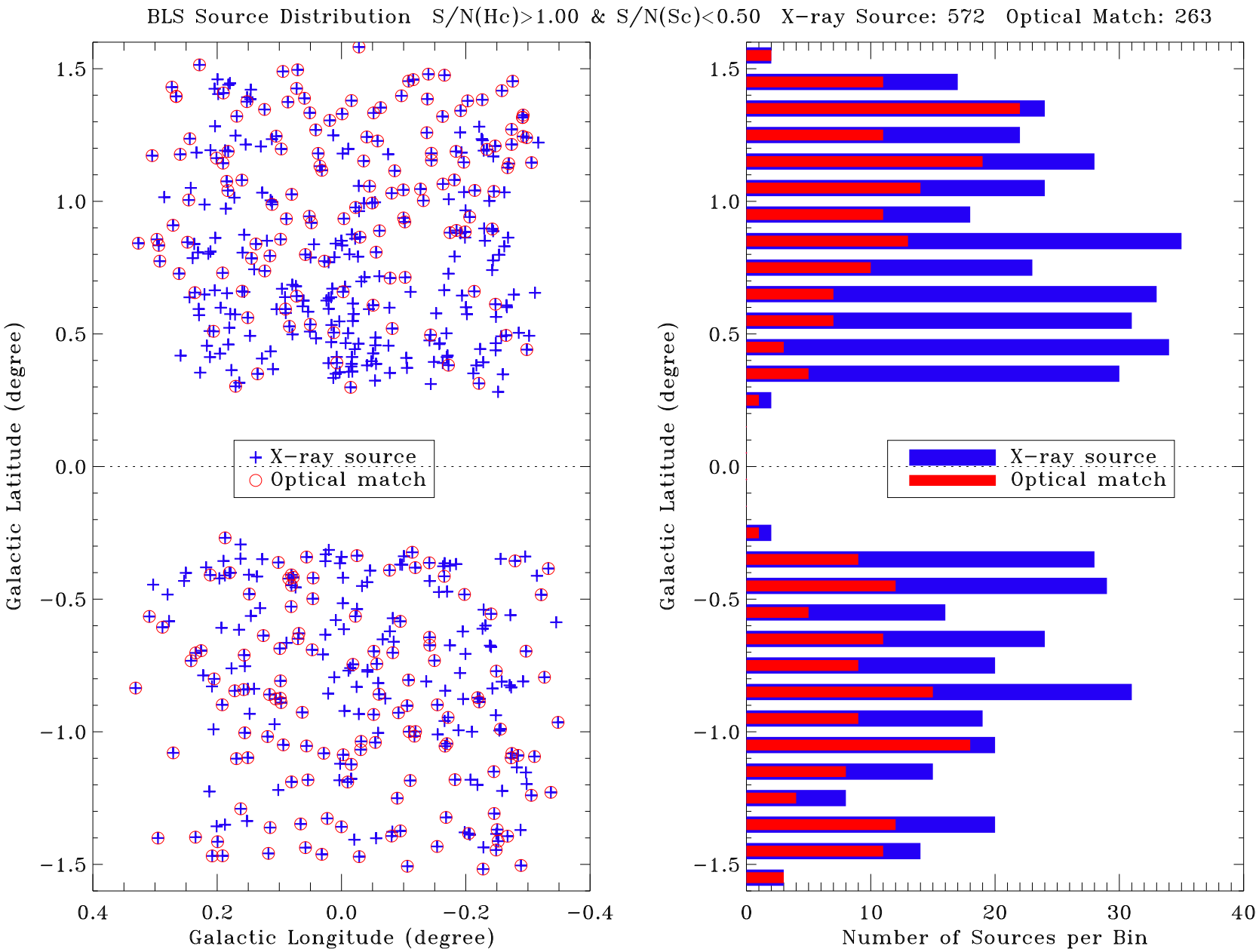

Figure 18: BLS source distribution: Hc (2.0–8.0keV) band sources without Sc (0.5–2.0keV) band emission. Source number decrease while moving away from the plane.

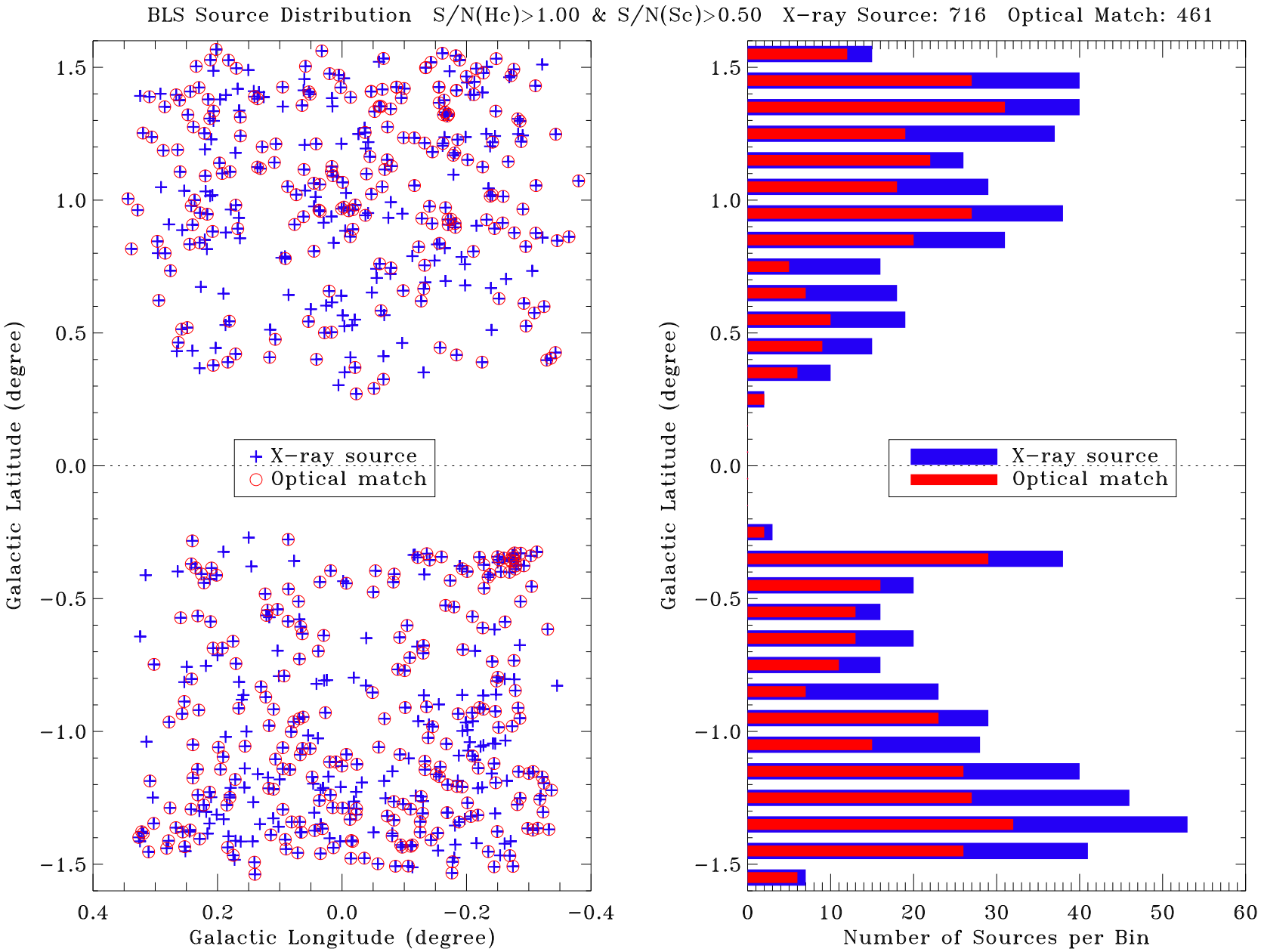

Figure 19: BLS source distribution: Hc (2.0–8.0keV) band sources with Sc (0.5–2.0keV) band emission. Source number increase while moving away from the plane, due to decreasing NH.

Summary

- **We have conducted ChaMPlane BLS survey which is 0.8 degrees wide and extends from ± 0.2 to ± 1.6 degrees along the galactic latitude, centered at the SgrA*.**
- **The survey includes 36 Chandra/ACIS-I pointings of 15ks each, covering a total of $\sim$2.4 square-degrees region**
- **Deep optical (V,R,I,Hα band) and IR images were obtained from CTIO/4m to cover the same region.**
- **A total of more than 2500 point X-ray sources were found in the survey.**
- **Optical and infrared counterparts are found for many Chandra sources.**
- **Spectral follow-ups are conducted on Chandra optical counterparts.**
- **The source distribution shows number of hard sources decrease and number of soft sources increase while moving aways from the plane. And percentage of counterparts found increase while moving aways from the plane.**